Cell Metabolism

CellPress

Forum

Reassessment of antibody-based detection of the murine T cell GLP-1 receptor

Chi Kin Wong,[1] Bernardo Yusta,[1] Jason C.L. Tong,[2] Johannes Broichhagen,[3] David J. Hodson,[2] and Daniel J. Drucker[1,*]
[1]Lunenfeld-Tanenbaum Research Institute, Mt. Sinai Hospital, Toronto, ON, Canada
[2]Oxford Centre for Diabetes, Endocrinology and Metabolism, Oxford Centre for Diabetes, Endocrinology and Metabolism (OCDEM), NIHR Oxford Biomedical Research Centre, Churchill Hospital, Radcliffe Department of Medicine, University of Oxford, Oxford, UK
[3]Leibniz-Forschungsinstitut für Molekulare Pharmakologie, Robert-Rössle-Straße 10, 13125 Berlin, Germany
*Correspondence: drucker@lunenfeld.ca
https://doi.org/10.1016/j.cmet.2025.06.012

Glucagon-like peptide 1 receptor (GLP-1R) agonists exhibit anti-inflammatory actions, yet the importance of direct immune cell GLP-1R signaling remains uncertain. Although T cells respond to GLP-1, low receptor abundance and suboptimal antisera complicate efforts to characterize immune cell GLP-1R signaling. Here, we evaluate three frequently utilized GLP-1R antibodies, revealing that one of several antibodies, AGR-021, lack ideal specificity for detecting the GLP-1R in mice. Immunostaining with AGR-021 using tissues from two independent GLP-1R knockout mouse lines reveals persistent immunoreactive signals in GLP-1R-null pancreatic islets. Similarly, flow cytometry using AGR-021 reveals no reduction in AGR-021 immunoreactivity in GLP-1R-null splenic T cells. Moreover, western blotting detects AGR-021-immunoreactive proteins from a GLP-1R-negative cell line and fails to detect immunoreactive GLP-1R of the correct size upon overexpression of the receptor. Our findings reveal caveats governing use of multiple widely used GLP-1R antibodies, reemphasizing the importance of rigorous antibody validation for inferring accurate GLP-1R expression.

Introduction

There is tremendous interest in understanding how and where glucagon-like peptide 1 (GLP-1)-based medicines exert their direct actions, including reduction of inflammation.[1] Localization of many G protein-coupled receptors (GPCRs), including the GLP-1R, at the protein level is challenging due to low-level expression and the scarcity of rigorously validated antibodies. In the intestine, mouse intraepithelial lymphocytes (IELs) are one of the few T cell populations that robustly express GLP-1R, with activity of these cells functionally suppressed by GLP-1R agonists (GLP-1RAs) in a receptor-dependent manner.[2,3] In contrast, immune organs such as the thymus, bone marrow, spleen, and peripheral lymph nodes express low levels of *Glp1r*.[2–5] Within these organs, *Glp1r* is likely expressed in subsets of immune cells, as inferred from studies using transgenic mice lacking *Glp1r* in Lck- or Tie2-expressing lineages.[2,6]

A recent preclinical study demonstrated that GLP-1R activation dampens T cell-mediated immune responses to promote tolerance, while its inhibition enhanced immune activity. A commercially available antibody (clone AGR-021, Alomone Labs), raised against the extracellular domain of rat GLP-1R, was used to detect immunoreactive GLP-1R expression in mouse and human T cells and to characterize GLP-1R^{+} versus GLP-1R^{-} T cells for cellular and molecular analyses.[7] However, several issues raise questions about the interpretation of data generated using the AGR-021 antibody. These include the very low levels of *Glp1r* mRNA in major immune organs[2–5] yet surprisingly widespread distribution of GLP-1R immunoreactive immune cells detected using AGR-021.[7] Second, western blot data using AGR-021 report a GLP-1R-immunoreactive band at 110 kDa, but not at the expected molecular weight of the GLP-1R at ~55 kDa.[8,9] Third, AGR-021 yields diffuse, non-membrane-associated staining in pancreatic regions that do not resemble islets.[10,11] Collectively, these observations suggest that AGR-021 immunoreactivity may not faithfully report authentic GLP-1R expression. Given preceding problems with the sensitivity and specificity of multiple GLP-1R antisera,[12] we used complementary methods across two independent laboratories to evaluate the suitability of AGR-021 for detecting mouse GLP-1R expression.

Results

AGR-021 immunoreactivity does not colocalize with fluorescent GLP-1R ligand signals in isolated mouse islets

We first performed immunofluorescence staining on isolated pancreatic islets from whole-body *Glp1r* knockout mice (*Glp1r*$^{H-KO}$) generated via CRISPR-Cas9.[11] Pancreatic islets express high levels of GLP-1R, which can be reliably visualized using LUXendin645, a fluorescent exendin-9-39 peptide probe that binds GLP-1R with high specificity.[11] As expected, LUXendin645 produced membrane-associated fluorescence in wild-type islet cells (Figure 1A).

We next tested the GLP-1R antibody ab218532, which showed strong colocalization with LUXendin645 in wild-type islets but no signal in GLP-1R-null islets (Figures 1A and 1B). Therefore, we used ab218532 as a control in subsequent experiments. In contrast, AGR-021 produced sparse and inconsistent staining across islet cells, showing minimal overlap with LUXendin645 (Figure 1C). Critically, AGR-021 generated diffuse cytoplasmic fluorescence signals in GLP-1R-null islets. In contrast, LUXendin645 did not label any

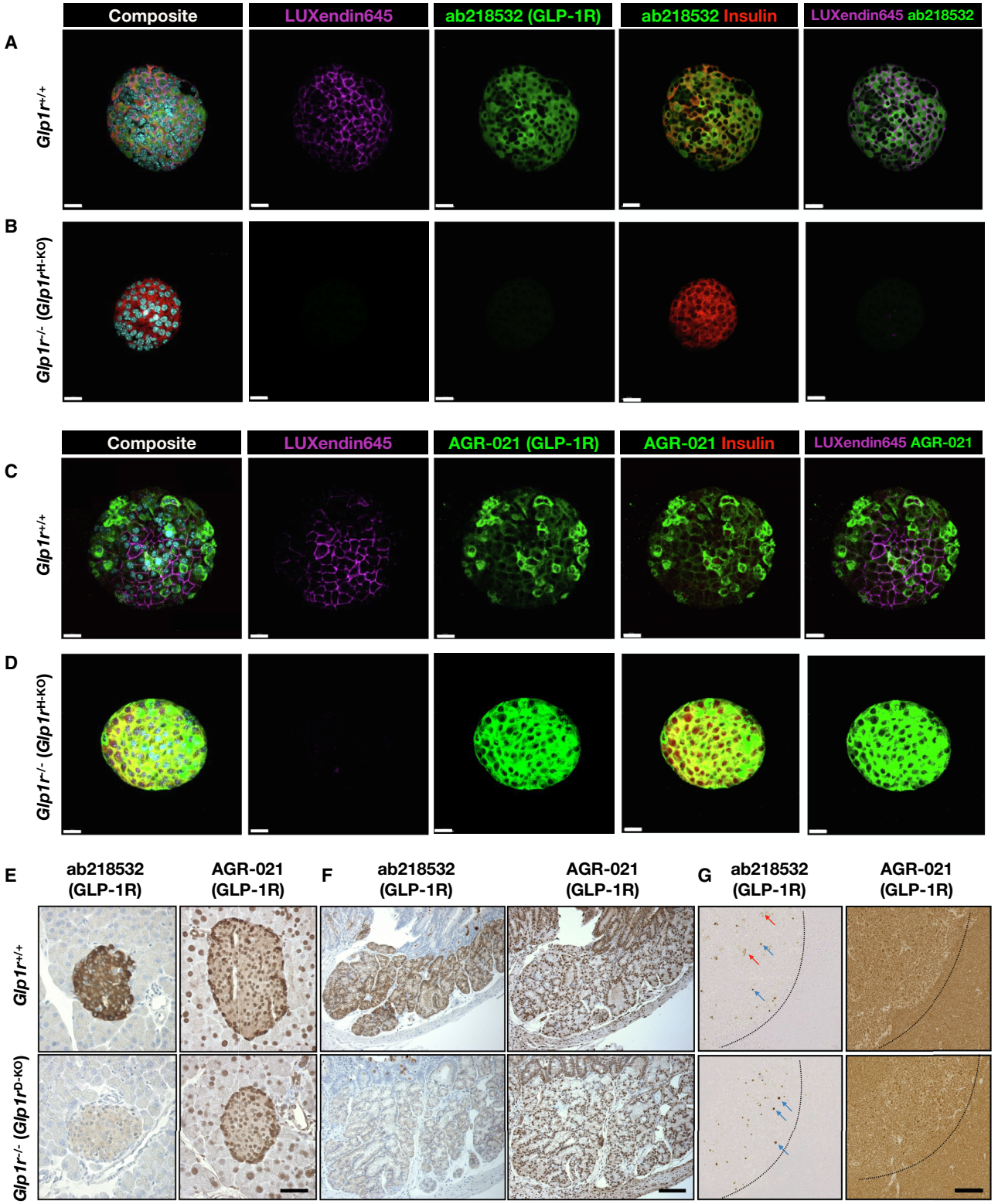

Figure 1. AGR-021 lacks specificity for detection of mouse GLP-1R by immunofluorescence and immunohistochemistry

(A and B) Isolated islets from (A) *Glp1r*$^{+/+}$ and (B) *Glp1r*$^{-/-}$ (*Glp1r*$^{H-KO}$) mice showing GLP-1R labeling with ab218532 (green), LUXendin645 (magenta), insulin (red), and Hoechst 33342 (cyan) by immunofluorescence. Scale bar, 20 μm. $n = 3$.

(legend continued on next page)

cells in GLP-1R-null islets (Figure 1D). Of note, insulin staining was much weaker in islets co-stained with AGR-021, suggesting some non-specific binding to, and competition for, insulin epitopes (Figure 1C).

AGR-021 immunoreactivity persists in tissues lacking GLP-1R

We next assessed AGR-021 and ab218532 on tissue sections from a second, independently generated whole-body GLP-1R knockout mouse line (*Glp1r*$^{D-KO}$).[13] In wild-type pancreas, ab218532 produced strong staining restricted to islets, with no detectable signals in the exocrine pancreas (Figure 1E). This staining was markedly reduced in the GLP-1R-null pancreas. In contrast, AGR-021 produced similar staining patterns in both wild-type and GLP-1R-null pancreata, with signals observed in both exocrine and endocrine compartments (Figure 1E). Within the islets, AGR-021 staining localized primarily to the mantle region, typically enriched in non-β cells in mice, suggesting that its staining does not reflect specific detection of GLP-1R.

We also tested antibody performance on Brunner's glands, which express high levels of GLP-1R. The ab218532 antibody mainly stained secretory cells with a membrane-associated pattern consistent with GLP-1R localization (Figure 1F).[14] Some non-specific staining was observed in mucus vacuoles of the gut epithelium in both wild-type and GLP-1R knockout mice. However, secretory cells in the duodenum of GLP-1R knockout mice lacked detectable ab218532 staining, supporting its specificity. In contrast, AGR-021 produced strong nuclear staining in both Brunner's glands and adjacent epithelium, with similar patterns in wild-type and GLP-1R-null tissues, indicating non-specific binding (Figure 1F).

We next tested these antibodies in mouse thymus sections, where AGR-021 was previously reported to label thymic cells with diffuse cytoplasmic GLP-1R immunopositivity.[7] In wild-type thymus, ab218532 showed sparse staining in the medulla and none in the cortex (Figure 1G). Two distinct cell populations were labeled: one with membrane-associated staining and another with strong cytoplasmic signal. In GLP-1R-null thymus, membrane-associated staining was absent, while cytoplasmic staining remained, suggesting that the cytoplasmic signals represent non-specific background (Figure 1G). In contrast, AGR-021 showed widespread staining across both cortex and medulla, with similar patterns observed in wild-type and GLP-1R-null tissues (Figure 1G). These findings indicate that AGR-021 lacks both sensitivity and specificity for detecting mouse GLP-1R by immunohistochemistry, whereas ab218532 demonstrates high sensitivity and moderate specificity across tissues.

Enrichment of AGR-021-immunoreactive splenic T cells

The AGR-021 antibody has been widely used to detect GLP-1R (Table S1), including in flow cytometry experiments to identify GLP-1R$^+$ splenic T cells for functional and transcriptomics analyses.[7,15] To further assess its specificity, we performed flow cytometry on live splenic T cells from wild-type and GLP-1R-null mice. AGR-021 labeled a small subset of both CD4$^+$ and CD8$^+$ splenic T cells relative to fluorescence-minus-one controls (Figures 2A and 2B). Importantly, the frequency of AGR-021$^+$ T cells was the same between wild-type and GLP-1R-null spleens, suggesting non-specific binding (Figure 2C). Given the very low level of *Glp1r* expression in spleen,[3,6,7] we tested whether AGR-021 could detect GLP-1R$^+$ T cells in gut IELs, a cell type that robustly expresses *Glp1r*.[2,3] Similar to splenocytes, AGR-021 bound similar fractions of CD8$^+$ IELs from wild-type and GLP-1R-null mice (Figure 2D). We also tested ab218532, which produced no flow cytometry signals on splenocytes (data not shown). Another commonly used monoclonal antibody, 7F38,[10] labeled small populations of splenic T cells and IELs, but the frequency of 7F38$^+$ T cells did not differ between wild-type and GLP-1R-null mice (Figures 2E and 2F).

To determine whether AGR-021$^+$ cells truly express *Glp1r*, we magnetically enriched CD90$^+$ splenic T cells and performed fluorescence-activated cell sorting (FACS) to isolate AGR-021$^+$ and AGR-021$^-$ CD4$^+$ and CD8$^+$ populations. CD90$^+$ splenic T cells expressed higher levels of *Glp1r* than bulk splenocytes by qPCR (Figure 2G). All sorted populations expressed high levels of *Cd3g*, although AGR-021$^+$ T cells exhibited lower levels of *Cd3g* than AGR-021$^-$ cells (Figure 2H). Interestingly, AGR-021$^+$ CD4$^+$ T cells expressed *Glp1r*, but AGR-021$^+$ CD8$^+$ T cells did not (Figure 2G). Together, these results suggest that AGR-021 lacks sufficient specificity for reliable detection of GLP-1R in mouse T cells by flow cytometry.

AGR-021 fails to detect mouse GLP-1R at the expected molecular weight

Finally, we examined the performance of AGR-021 and ab218532 by western blotting from cells overexpressing mouse GLP-1R (Figure 2I) as previously described.[9] Probing with AGR-021 produced multiple (at least six) bands in both control and GLP-1R-overexpressing cell lysates (Figure 2I). Although a 110 kDa band was visible with AGR-021 as previously reported,[7] there was no signal at 55 kDa, the expected molecular weight of mouse GLP-1R.[9] In contrast, ab218532 produced a strong 55 kDa band only in GLP-1R-overexpressing cells with no such band in control lysates (Figure 2I). GAPDH levels were consistent across samples (Figure 2I). These results demonstrate that AGR-021 lacks both sensitivity and specificity for detecting mouse GLP-1R by western blotting.

Discussion

Detecting native GPCRs using antibodies remains challenging due to their typically low and variable cell surface expression, coupled with difficulties stabilizing the receptors for the generation of specific antibodies. Many commercially available GPCR-targeting antibodies lack sufficient sensitivity and specificity, and several GLP-1R antibodies have been invalidated using tissues from GLP-1R knockout mice.[9,12] The widespread use of GLP-1R antibodies that lack specificity raises

(C and D) Isolated islets from (C) *Glp1r*$^{+/+}$ and (D) *Glp1r*$^{-/-}$ mice showing GLP-1R labeling with AGR-021 (green), LUXendin645 (magenta), insulin (red), and Hoechst 33342 (cyan) by immunofluorescence. Scale bar, 20 μm. $n = 3$.
(E–G) Immunohistochemistry staining of ab218532 or AGR-021 in the (E) mouse pancreas, (F) Brunner's gland, and (G) thymus, counterstained with hematoxylin. Blue arrows designate cells with cytoplasmic staining; red arrows denote cells with membrane staining. Scale bar, 50 μm (E) and 100 μm (F and G). $n = 4$ from two independent experiments.

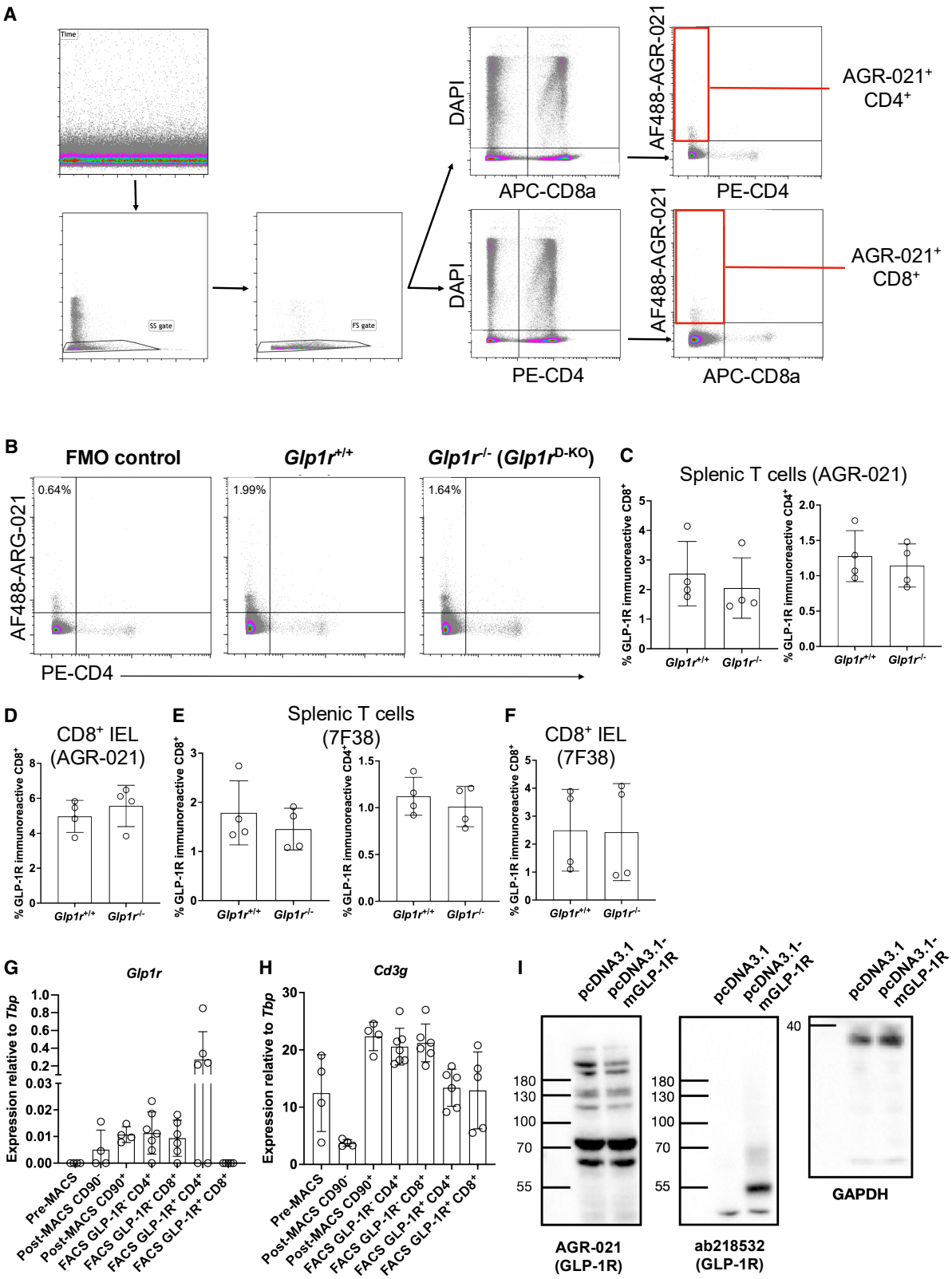

(legend on next page)

significant concerns about the reproducibility and reliability of data implying localization of the GLP-1R, a drug target of expanding importance.

Here, we found that the AGR-021 antibody is neither specific nor sensitive for detecting mouse GLP-1R, using commonly used techniques such as immunofluorescence, immunohistochemistry, flow cytometry, and western blotting. AGR-021 performed poorly relative to ab218532, which we validated for several applications except flow cytometry. AGR-021 lacks specificity, as it produces signals even in GLP-1R-null tissues and in cell lines that do not express the GLP-1R. It also lacks sensitivity, failing to produce membrane-associated staining in pancreatic β cells and failing to detect a 55 kDa band in western blotting, even in extracts from transfected cells with high levels of GLP-1R expression.

Our findings further underscore that the performance of GLP-1R antibodies is highly assay and tissue dependent. For example, ab218532 is reasonably suitable for immunohistochemistry, immunofluorescence, and western blotting but is ineffective in flow cytometry. Similarly, 7F38 was validated for immunohistochemistry to detect GLP-1R in islets but lacks the sensitivity and specificity required for flow-based applications and has not been reliably validated for western blotting. Notably, 7F38 is a mouse-derived monoclonal antibody, which complicates its use in mouse tissues due to potential cross-reactivity and increased background when paired with anti-mouse secondary antibodies. Moreover, the very low expression of *Glp1r* in the spleen and thymus challenges the sensitivity of flow-based detection. Although ab218532 showed minimal signals in the Brunner's glands, pancreatic islet, and thymus of GLP-1R-null mice in immunohistochemistry experiments, some background staining was still observed. This highlights that even relatively specific antibodies can produce non-specific signals under certain experimental conditions. Therefore, validation of GLP-1R detection should include orthogonal methods, such as *in situ* hybridization or fluorescently labeled GLP-1R ligands (e.g., LUXendin probes), used in conjunction with multiple knockout tissues to ensure specificity.

Given the lack of specificity of AGR-021, it remains unclear whether peripheral conventional T cells express GLP-1R at functionally meaningful levels. We observed higher *Glp1r* transcript levels in CD90$^+$ splenocytes than in CD90$^-$ cells, suggesting that T cells may contribute a greater share of splenic *Glp1r* expression. In addition, AGR-021$^+$ CD4$^+$ T cells showed enrichment of *Glp1r* transcripts, whereas AGR-021$^+$ CD8$^+$ T cells did not. It is possible that AGR-021 binds an unrelated antigen expressed by a subset of T cells that coincidentally also express *Glp1r*, rather than specifically recognizing GLP-1R. We interpret this enrichment as coincidental for several reasons: (1) AGR-021 fails specificity and sensitivity tests across immunohistochemistry, immunofluorescence, and western blotting; (2) it produces flow cytometry signals in GLP-1R-null splenic T cells and IELs; and (3) AGR-021$^-$ CD4$^+$ and AGR-021$^-$ CD8$^+$ T cells still express detectable *Glp1r* transcripts. These findings suggest that a subset of CD4$^+$ T cells may genuinely express *Glp1r*, independent of AGR-021 staining. Notably, CD4$^+$ splenic T cells expressing high levels of *Glp1r* transcripts may include regulatory T cells (Tregs), one of the few splenic immune populations known to express full-length *Glp1r* mRNA[4] and a plausible target through which GLP-1R signaling could modulate immune tolerance.

Assessment of how GLP-1 medicines directly modify GLP-1R signaling in immune cells has important translational implications for understanding the safety and anti-inflammatory actions of GLP-1 medicines across a range of human diseases. Although several studies describe exciting actions for GLP-1 medicines in the modulation of experimental T cell function, the use of the AGR-021 antibody to isolate and identify putative GLP-1R$^+$ T cells in these studies[7,15] is challenged by the major limitations of this reagent identified herein. Our findings suggest that key conclusions relying on AGR-021 for detecting GLP-1R-positive T cells should be re-evaluated using validated antibodies and orthogonal methods. Reproduction of these observations with rigorously validated reagents will be necessary to confirm the role of GLP-1R in T cell biology. Taken together, our data reinforce the ongoing importance of vigilance and thorough reagent validation using multiple techniques, especially in a field experiencing intense scientific and public scrutiny, to ensure accuracy and reproducibility in studies assessing GLP-1R localization, expression, and function.

Limitations of the study

A limitation of our flow cytometry experiments is the absence of isotype and blocking peptide controls, which are useful for assessing non-specific antibody binding.

Figure 2. AGR-021 fails to detect mouse GLP-1R by flow cytometry and western blotting

(A) Gating strategies for AGR-021$^+$ splenic T cells. Forward and side scatter properties were used to gate singlet events (SS and FS gates). Singlet events were gated further by DAPI and CD8a or CD4 to identify DAPI$^-$ CD8$^+$ (live CD8$^+$ T cells) or DAPI$^-$ CD4$^+$ (live CD4$^+$ T cells). GLP-1R signals (AGR-021) were gated on these live T cells.

(B) Representative density plots of CD8$^+$ splenic T cells stained with AGR-021 and CD4. AGR-021$^+$ CD4$^-$ populations (the gate with numeric percentages shown) were quantified. Data are gated on DAPI$^-$ CD8$^+$ populations.

(C) Bar plots showing the frequencies of AGR-021$^+$ CD8$^+$ CD4$^-$ (left) and AGR-021$^+$ CD8$^-$ CD4$^+$ (right) splenic T cells. n = 4. Data are pooled from two independent experiments.

(D) Bar plots showing the frequencies of AGR-021$^+$ CD8$^+$ CD4$^-$ IELs. n = 4. Data are pooled from two independent experiments.

(E) Bar plots showing the frequencies of 7F38$^+$ CD8$^+$ CD4$^-$ (left) and 7F38$^+$ CD8$^-$ CD4$^+$ (right) splenic T cells. n = 4. Data are pooled from two independent experiments.

(F) Bar plots showing the frequencies of 7F38$^+$ CD8$^+$ CD4$^-$ IELs. n = 4. Data are pooled from two independent experiments.

(G and H) qPCR analysis of (G) *Glp1r* and (H) *Cd3g* expression in pre-MACS (bulk splenocytes), MACS-purified CD90$^+$ and CD90$^-$ cells, and FACS-purified AGR-021$^-$ or AGR-021$^+$ CD4$^+$ and CD8$^+$ T cells. n = 4–6. Data are pooled from three independent experiments.

(I) Western blot detection of overexpressed mouse GLP-1R using AGR-021 and ab218532 antibodies. Lysates of cells transfected with either empty vector (pcDNA3.1) or pcDNA3.1 containing full-length mouse *Glp1r* cDNA were probed with AGR-021, ab218532, or anti-GAPDH as a loading control. The experiment was independently repeated twice.

Data are represented as mean ± standard deviation.

FMO, fluorescence-minus-one; MACS, magnetic-activated cell sorting; FACS, fluorescence-activated cell sorting.

Nevertheless, the inclusion of GLP-1R knockout tissues provides a more biologically relevant control that strongly supports our conclusions about antibody specificity. In addition, although qPCR is a sensitive technique for detecting transcripts in samples with a low number of cells, *Glp1r* gene expression detected by qPCR is not always indicative of GLP-1R protein expression. Moreover, we focused our validation studies here on detection of the mouse GLP-1R, and the conclusions made here cannot be generalized across species. Furthermore, it is possible that under some circumstances, cell-specific post-translational modification of the GLP-1R may diminish recognition using reasonably well-validated antibodies, further challenging conclusions drawn from antibody validation using a limited number of tissues and conditions.

ACKNOWLEDGMENTS

D.J.D. is supported, in part, by a Banting and Best Diabetes Centre–Novo Nordisk Chair in Incretin Biology, a Sinai Health–Novo Nordisk Foundation Fund in Regulatory Peptides, CIHR grants 154321 and 19204, and Diabetes Canada-Canadian Cancer Society grant (OG-3-24-5819-DD). This project has received funding from the European Union's Horizon Europe Framework Programme (deuterON, grant agreement no. 101042046 to J.B.). D.J.H. was supported by MRC (MR/S025618/1), Diabetes UK (22/0006389), and UKRI ERC Frontier Research Guarantee (EP/X026833/1). This work was supported on behalf of the "Steve Morgan Foundation Type 1 Diabetes Grand Challenge" by Diabetes UK and SMF (grant number 23/0006627 to J.B. and D.J.H.).

DECLARATION OF INTERESTS

D.J.D. has received consulting fees from Alnylam, Amgen, AstraZeneca Inc., Crinetics, Eli Lilly, Insulet, Kallyope, Metsara, and Pfizer Inc. and speaking fees from Novo Nordisk Inc. Mt. Sinai Hospital receives investigator-initiated grant support from Amgen, Eli Lilly Inc., Novo Nordisk, Pfizer, and Zealand Pharmaceuticals Inc. to support preclinical studies in the Drucker laboratory. J.B. and D.J.H. have filed a patent on GLP-1R and GIPR chemical probes. J.B. and D.J.H. receive licensing revenue from Celtarys Research for provision of GLP-1R/GIPR chemical probes. D.J.H. has filed patents related to type 2 diabetes therapy and GLP-1R agonism.

SUPPLEMENTAL INFORMATION

Supplemental information can be found online at https://doi.org/10.1016/j.cmet.2025.06.012.

REFERENCES

1. Drucker, D.J. (2024). The benefits of GLP-1 drugs beyond obesity. Science *385*, 258–260. https://doi.org/10.1126/science.adn4128.

2. Wong, C.K., Yusta, B., Koehler, J.A., Baggio, L. L., McLean, B.A., Matthews, D., Seeley, R.J., and Drucker, D.J. (2022). Divergent roles for the gut intraepithelial lymphocyte GLP-1R in control of metabolism, microbiota, and T cell-induced inflammation. Cell Metab. *34*, 1514–1531.e7. https://doi.org/10.1016/j.cmet.2022.08.003.

3. Yusta, B., Baggio, L.L., Koehler, J., Holland, D., Cao, X., Pinnell, L.J., Johnson-Henry, K. C., Yeung, W., Surette, M.G., Bang, K.W.A., et al. (2015). GLP-1 receptor (GLP-1R) agonists modulate enteric immune responses through the intestinal intraepithelial lymphocyte GLP-1R. Diabetes. *64*, 2537–2549. https://doi.org/10.2337/db14-1577.

4. Hadjiyanni, I., Siminovitch, K.A., Danska, J.S., and Drucker, D.J. (2010). Glucagon-like peptide-1 receptor signalling selectively regulates murine lymphocyte proliferation and maintenance of peripheral regulatory T cells. Diabetologia *53*, 730–740.

5. McLean, B.A., Wong, C.K., Campbell, J.E., Hodson, D.J., Trapp, S., and Drucker, D.J. (2021). Revisiting the complexity of GLP-1 action from sites of synthesis to receptor activation. Endocr. Rev. *42*, 101–132. https://doi.org/10.1210/endrev/bnaa032.

6. McLean, B.A., Wong, C.K., Kaur, K.D., Seeley, R. J., and Drucker, D.J. (2021). Differential importance of endothelial and hematopoietic cell GLP-1Rs for cardiometabolic versus hepatic actions of semaglutide. JCI Insight *6*, e153732. https://doi.org/10.1172/jci.insight.153732.

7. Ben Nasr, M., Usuelli, V., Dellepiane, S., Seelam, A.J., Fiorentino, T.V., D'Addio, F., Fiorina, E., Xu, C., Xie, Y., Balasubramanian, H.B., et al. (2024). Glucagon-like peptide 1 receptor is a T cell-negative costimulatory molecule. Cell Metab. *36*, 1302–1319.e12. https://doi.org/10.1016/j.cmet.2024.05.001.

8. Baggio, L.L., Yusta, B., Mulvihill, E.E., Cao, X., Streutker, C.J., Butany, J., Cappola, T.P., Margulies, K.B., and Drucker, D.J. (2018). GLP-1 receptor expression within the human heart. Endocrinology *159*, 1570–1584. https://doi.org/10.1210/en.2018-00004.

9. Panjwani, N., Mulvihill, E.E., Longuet, C., Yusta, B., Campbell, J.E., Brown, T.J., Streutker, C., Holland, D., Cao, X., Baggio, L. L., and Drucker, D.J. (2013). GLP-1 receptor activation indirectly reduces hepatic lipid accumulation but does not attenuate development of atherosclerosis in diabetic male ApoE-/- mice. Endocrinology *154*, 127–139. https://doi.org/10.1210/en.2012-1937.

10. Jensen, C.B., Pyke, C., Rasch, M.G., Dahl, A.B., Knudsen, L.B., and Secher, A. (2018). Characterization of the glucagonlike peptide-1 receptor in male mouse brain using a novel antibody and in situ hybridization. Endocrinology *159*, 665–675. https://doi.org/10.1210/en.2017-00812.

11. Ast, J., Arvaniti, A., Fine, N.H.F., Nasteska, D., Ashford, F.B., Stamataki, Z., Koszegi, Z., Bacon, A., Jones, B.J., Lucey, M.A., et al. (2020). Super-resolution microscopy compatible fluorescent probes reveal endogenous glucagon-like peptide-1 receptor distribution and dynamics. Nat. Commun. *11*, 467. https://doi.org/10.1038/s41467-020-14309-w.

12. Ast, J., Broichhagen, J., and Hodson, D.J. (2021). Reagents and models for detecting endogenous GLP1R and GIPR. EBioMedicine *74*, 103739. https://doi.org/10.1016/j.ebiom.2021.103739.

13. Scrocchi, L.A., Brown, T.J., MaClusky, N., Brubaker, P.L., Auerbach, A.B., Joyner, A.L., and Drucker, D.J. (1996). Glucose intolerance but normal satiety in mice with a null mutation in the glucagon-like peptide 1 receptor gene. Nat. Med. *2*, 1254–1258. https://doi.org/10.1038/nm1196-1254.

14. Pyke, C., Heller, R.S., Kirk, R.K., Ørskov, C., Reedtz-Runge, S., Kaastrup, P., Hvelplund, A., Bardram, L., Calatayud, D., and Knudsen, L.B. (2014). GLP-1 receptor localization in monkey and human tissue; novel distribution revealed with extensively validated monoclonal antibody. Endocrinology *155*, 1280–1290. https://doi.org/10.1210/en.2013-1934.

15. Wu, J., Qian, P., Han, Y., Xu, C., Xia, M., Zhan, P., Wei, J., and Dong, J. (2025). GLP1 alleviates oleic acid-propelled lipocalin-2 generation by tumor-infiltrating $CD8^+$ T cells to reduce polymorphonuclear MDSC recruitment and enhances viral immunotherapy in pancreatic cancer. Cell. Mol. Immunol. *22*, 282–299. https://doi.org/10.1038/s41423-025-01260-3.

Cell Metabolism, Volume *37*

Supplemental information

Reassessment of antibody-based detection of the murine T cell GLP-1 receptor

Chi Kin Wong, Bernardo Yusta, Jason C.L. Tong, Johannes Broichhagen, David J. Hodson, and Daniel J. Drucker

Supplementary Table 1. Summary of published studies using the rabbit anti-GLP-1R AGR-021 antibody.

Authors	PMID	Applications	Species Detected	Tissues Detected	Validation
Wu et al 2025 *Cell Mol Immunol*	39910336	Flow cytometry	Mouse	Splenic, blood, tumor $CD8^+$ T cells	None
Wu et al 2025 *Cell Mol Immunol*	39910336	Western blotting	Mouse	OT-1 $CD8^+$ T cells	None
Nasr et al 2024 *Cell Metab*	38838642	Flow cytometry	Mouse/Human	Splenic T cells	None
Nasr et al 2024 *Cell Metab*	38838642	Immunohistochemistry	Mouse/Human	Pancreas, thymus	None
Nasr et al 2024 *Cell Metab*	38838642	Western blotting	Mouse	Heart, islets	*Glp1r*$^{-/-}$ mouse islets/heart tissues
Kanemaru et al 2023 *Nature*	37438528	Immunofluorescence	Human	iPSC-derived cardiomyocytes	None
Nakamori et al 2021 Am J Physiol Gastrointest Liver Physiol	34643099	Immunofluorescence	Rat	Colonic myenteric plexuses	Blocking peptide by immunofluorescence
Zatorski et al 2021 *Pharmacol Rep*	34535873	Western Blotting	Mouse	Colon	None
Chilelli et al 2021 Am J Physiol Endocrinol Metab	33779307	Immunofluorescence	Mouse	3T3-L1 cells	None
Peiris et al 2018 Nurtrients	30336615	Immunofluorescence	Mouse	Colonic crypts	None
Yang et al 2016 Theranostics	27698937	Western blotting	Rat	Primary cortical neurons	None
Gleizes et al 2016 J Cell Mol Med	26607759	Western blotting	Rat	Rin-m5f insulinoma cells	None
Gao et al 2012 J Nucl Med	23139087	Immunofluorescence	Rat	Heart	None

STAR★Methods

Key resources table

REAGENT or RESOURCE	SOURCE	IDENTIFIER
Antibodies		
Guinea pig anti-insulin	Dako	CAT: A056401-2-2; RRID: AB_2617169
Mouse anti-glucagon	Sigma-Aldrich	CAT: G2654; RRID: AB_2617169
Rabbit anti-GLP-1R	abcam	CAT: ab218532; RRID: AB_2864762
Rabbit anti-GLP-1R	Alomone Labs	CAT: AGR-021; RRID: AB_10917158
Alexa Fluor 488-conjugated donkey anti-rabbit IgG	Thermo Fisher	CAT: A-21206; RRID: AB_2535792
Alexa Fluor 568-conjugated donkey anti-guinea pig IgG	Thermo Fisher	CAT: A-11075; RRID: AB_2534119
Alexa Fluor 647-conjugated donkey anti-mouse IgG	abcam	CAT: ab150119; RRID: AB_2811129
Purified anti-CD16/32	Biolegend	CAT: 101302; RRID: AB_312801
Mouse anti-GLP-1R (7F38)	Custom synthesis by Novo Nordisk	N/A
Alexa Fluor 488-conjugated donkey anti-mouse IgG	abcam	CAT: ab150105; RRID: AB_2732856
PE anti-CD4	Biolegend	CAT: 100512; RRID: AB_312715
APC anti-CD8a	Biolegend	CAT: 100712; RRID: AB_312751
Rabbit anti-GAPDH	Cell Signaling Technology	CAT: 2118; RRID: AB_561053
Anti-rabbit IgG, HRP-linked Antibody	Cell Signaling Technology	CAT: 7074; RRID: AB_2099233
Chemicals, peptides, and recombinant proteins		
LUXendin-645	Custom synthesis	N/A

Hoechst 33342	Thermo Fisher	CAT: H3570
ProLong Glass Antifade Mountant	Thermo Fisher	CAT; P36982
Goat serum	Sigma-Aldrich	CAT; G9023
SignalStain Boost IHC Detection Reagent (HRP, Rabbit)	Cell Signaling Technology	CAT: 8114
ImmPACT DAB Substrate Kit, Peroxidase	Vector Laboratories	CAT: SK-4105
ProLong Gold Antifade Mountant	Thermo Fisher	CAT: P36934
Hematoxylin QS	Vector Laboratories	CAT: H-3404-100
Fetal bovine serum	Wisent Bioproducts	CAT: 080-150
RPMI 1640	Wisent Bioproducts	CAT: 350-000-EL
Penicillin-Streptomycin, 100x	Thermo Fisher	CAT: 15140148
FcR blocking reagent, mouse	Miltenyi	CAT: 130-092-575
CD90.2 MicroBeads, mouse	Miltenyi	CAT: 130-121-278
LS columns	Miltenyi	CAT: 130-042-401
Percoll	Cytiva	CAT: 17089101
SuperScript III Reverse Transcriptase	Thermo Fisher	CAT: 18080085
TaqMan Fast Advanced Master Mix	Thermo Fisher	CAT: 4444965
DAPI	Thermo Fisher	CAT: 62248
SuperSignal West Pico PLUS chemiluminescent substrate	Thermo Fisher	CAT: 34577
Experimental models: Organisms/strains		
Mouse: C57BL/6J	Jackson Laboratory	CAT: 000664; RRID: IMSR_JAX:000664

Mouse: *Glp1r*$^{H-KO}$	In house[S1]	N/A
Mouse: *Glp1r*$^{D-KO}$	In house[S2]	N/A
Oligonucleotides		
Glp1r Taqman assays	Thermo Fisher	Mm00445292_m1
Cd3g Taqman assays	Thermo Fisher	Mm00438095_m1
Tbp Taqman assays	Thermo Fisher	Mm00446973_m1
Software and algorithms		
GraphPad Prism 9	GraphPad	RRID: SCR_002798
Kaluza 2.1	Beckman Coulter	RRID: SCR_016182
Other		
Teklad global 18% protein rodent diets (regular chow)	Envigo	CAT: 2018

Resource availability

Lead contact

Lead contact Daniel J. Drucker (drucker@lunenfeld.ca) is the lead contact and takes full responsibility for the data in this paper.

Materials availability

Materials and reagents are available from the lead contact upon reasonable request. No unique reagents or materials were generated in these studies.

Data and code availability

No proprietary data or code is associated with this manuscript. Any additional information required to reanalyze the data reported in this paper is available from the lead contact upon request.

Experimental model and study participant details

Animal studies

All animal procedures were approved by the Animal Care and Use Subcommittee at the Toronto Centre for Phenogenomics at Mount Sinai Hospital (Toronto, Canada), and were also approved by the University of Oxford Animal Welfare and Ethical Review Body (AWERB), and regulated by the Animals (Scientific Procedures) Act 1986 of the U.K. (Personal Project Licence PP1778740). Mice were housed in groups of up to five per cage in holding rooms with lights on between 7 a.m. and 7 p.m., with *ad libitum* access to water and standard chow. *Glp1r*$^{H-KO}$ mice

were generated using a CRISPR-Cas9 approach,[S1] and *Glp1r*$^{D-KO}$ mice were produced by traditional homologous recombination.[S2]

Method details

LUXendin-based GLP-1R labeling and immunofluorescence staining of mouse islets

Size-matched islets were incubated with LUXendin645 (500 nM) for 1 h at 37°C in 5% CO_2 as previously described.[S1] Following labeling, islets were fixed in 10% formalin at room temperature for 15 min. Fixed islets were then incubated at 4°C overnight with primary antibodies diluted in blocking buffer (2% BSA, 0.2% Triton X-100 in PBS), followed by incubation with secondary antibodies in the same buffer. Nuclei were stained with 1 µg/mL Hoechst 33342 (Thermo Fisher) for 15 min before mounting with ProLong Glass Antifade Mountant (Thermo Fisher). The primary antibodies used included: guinea pig anti-insulin at 1/5 (Dako), mouse anti-glucagon at 1/2000 (Sigma-Aldrich), rabbit anti-GLP-1R at 1/1000 (ab218532; abcam) and rabbit anti-GLP-1R at 1/200 (AGR-021; Alomone Labs). Secondary antibodies included: donkey anti-rabbit Alexa Fluor 488 at 1/1000 (Thermo Fisher), goat anti-guinea pig Alexa Fluor 568 at 1/1000 (Thermo Fisher), and goat anti-mouse Alexa Fluor 647 at 1/1000 (abcam). Imaging was performed using an Olympus FV4000 confocal microscope equipped with highly sensitive SilVIR spectral detectors and 40x, 0.95 NA and 60x, 1.42 NA UPLSAPO oil immersion objectives. Identical laser power and detector % were used for all samples, with brightness and contrast adjustments applied equally for presentation purposes.

Immunohistochemistry

Pancreas, Brunner's gland, and thymus tissues were fixed in 10% formalin at room temperature for 24 h, followed by serial dehydration in ethanol and xylene. Dehydrated tissues were embedded in paraffin and sectioned at a thickness of 4 µm. Sections were rehydrated with xylene, ethanol, and water, then subjected to antigen retrieval in TE pH 9.0 at 95°C for 40 min in a Biocare decloaking chamber. After cooling, sections were then blocked with blocking buffer (10% goat serum and 0.1% Triton X-100 in TBST) at room temperature for 30 min. Primary antibodies were applied overnight at 4°C. Slides were then washed three times 5 min each in TBST, followed by incubation with horseradish peroxidase (HRP)-based SignalStain Boost IHC Detection Reagent (Cell Signaling Technology) at room temperature for 1 h. Primary antibodies used were rabbit anti-GLP1R ab218532 at 1/500 (abcam) and rabbit anti-GLP1R AGR-021 at 1/200 (Alomone Labs). After a further three washes in TBST, chromogenic signal development was performed using the Impact DAB substrate kit (Vector Laboratories) for 2 min. Slides were counterstained with hematoxylin QS diluted 1:10 in water for 30 s (Vector Laboratories), mounted with Prolong Gold Antifade Mountant (Thermo Fisher), and scanned at 20× magnification using a Zeiss Axioscan 7 slide scanner.

Magnetic cell sorting of CD90$^+$ splenic T cells

Splenocytes were isolated by gently mashing spleens through a 70-µm cell strainer with a syringe plunger into RPMI 1640 medium (Wisent) supplemented with 10% fetal bovine serum (FBS; Wisent) and penicillin/streptomycin (Thermo Fisher). Cells were washed once with RPMI,

then incubated on ice with mouse FcR blocking reagent (Miltenyi) for 10 min. Magnetic separation was performed using anti-CD90.2 microbeads (Miltenyi) and LS columns (Miltenyi) according to the manufacturer's protocol. The enriched $CD90^+$ splenic T cells were subsequently used for flow cytometry or FACS experiments.

Isolation of intraepithelial lymphocytes (IELs)

IELs were isolated from the small intestine as previously described.[S3] Small intestines were cut into 1-cm pieces, washed with HBSS without calcium/magnesium, and incubated in RPMI 1640 supplemented with 10% FBS (Wisent) and penicillin/streptomycin, 10 mM HEPES, and 1 mM DTT at 37°C for 40 min. Tissues were then centrifuged at 500 g for 5 min and resuspended in 10 mL of the same supplemented RPMI without DTT. The samples vortexed vigorously for 3 min, and the supernatant was collected by passing through a 100-µm cell strainer. The tissues remaining on the strainer were furthered vortexed in 10 mL medium and filtered again through the 100-µm cell strainer. The combined supernatant was top up to 40 mL with medium and centrifuged at 500 g for 5 min. The cell pellet was resuspended in 8 mL of 36% Percoll (GE Healthcare) and carefully layered over 67% Percoll (GE Healthcare). The gradient was centrifuged at 700 g for 20 min without acceleration or brake. Cells at the interface were collected, washed once with FACS buffer (25 mM HEPES, 2 mM EDTA, 1% FBS in PBS), and resuspended in FACS buffer. Percoll-purified IELs were sorted on an MA800 cell sorter (Sony) equipped with a 100-µm nozzle, using forward and side scattering profiles and DAPI (Thermo Fisher) to gate live lymphocytes. The sorted IEL population was consistently >90% viable and >90% $CD3^+$ and was used for subsequent flow cytometry experiments.

Flow cytometry and fluorescence-activated cell sorting (FACS)

Splenic T cells or IELs were adjusted to 1 x 10^6 cells/100 µL and blocked with anti-CD16/CD32 antibody (Biolegend) on ice for 10 min. Cells were then incubated with on ice for 30 min with 3 µg of one of the following antibodies diluted in FACS buffer: rabbit anti-GLP1R AGR-021 (Alomone Labs), mouse anti-GLP1R 7F38 (Novo Nordisk), or rabbit anti-GLP1R ab218532 (abcam). After washing with FACS buffer, cells were incubated on ice for 30 min with Alexa Fluor 488-conjugated anti-rabbit IgG or anti-mouse IgG secondary antibodies (Thermo Fisher), along with PE-conjugated anti-CD4 (Biolegend) and APC-conjugated anti-CD8a antibodies (Biolegend). Following a final wash, cells were stained with DAPI and analyzed on a Gallios cytometer (Beckman Coulter). Data analysis was performed using Kaluza Analysis 2.1 software (Beckman Coulter). For FACS sorting, AGR-021-stained splenic T cells were sorted on a Sony MA900 cell sorter into $AGR\text{-}021^+$ and $AGR\text{-}021^-$ $CD4^+$ and $CD8^+$ T cell populations. Sorted cells were lyzed in TRIzol and total RNA was extracted with a standard chloroform and ethanol extraction protocol, followed by cDNA synthesis using SuperScript III (Thermo Fisher) and analysis by quantitative PCR using Taqman assays (ThermoFisher) on a QuantStudio 5 instrument (Thermo Fisher). Relative expression was calculated using the 2-ΔΔCT method with *Tbp* as the reference gene.

Western blotting

BHK cells transfected with a pcDNA3.1 construct containing full-length mouse *Glp1r* cDNA were previously described.[S4] Cells were lysed in Laemmli buffer and incubated at 37°C for 1 h. Lysates containing 30 µg of total protein were resolved on 4–10% SDS-PAGE gels at 100 V.

Proteins were transferred onto PVDF membranes at a constant current of 350 mA and 4°C for 90 min. Membranes were blocked with 5% BSA in TBST, followed by overnight incubation at 4°C with primary antibodies diluted in blocking buffer. Primary antibodies included rabbit anti-GLP1R ab218532 at 1/1000 (Abcam), rabbit anti-GLP1R AGR-021 at 1/1000 (Alomone Labs), and rabbit anti-GAPDH at 1/2000 (CST). Blots were washed three times with TBST and incubated with HRP-conjugated anti-rabbit IgG secondary antibody (CST) at room temperature for 1 h. After three additional washes, membranes were incubated with SuperSignal West Pico PLUS chemiluminescent substrate (Thermo Fisher) for 5 min and imaged using a Bio-Rad ChemiDoc imaging system with exposure time up to 2 min.

Supplemental references

S1. Ast, J., Arvaniti, A., Fine, N.H.F., Nasteska, D., Ashford, F.B., Stamataki, Z., Koszegi, Z., Bacon, A., Jones, B.J., Lucey, M.A., et al. (2020). Super-resolution microscopy compatible fluorescent probes reveal endogenous glucagon-like peptide-1 receptor distribution and dynamics. Nat. Commun. *11*, 467. 10.1038/s41467-020-14309-w.

S2. Scrocchi, L.A., Brown, T.J., MaClusky, N., Brubaker, P.L., Auerbach, A.B., Joyner, A.L., and Drucker, D.J. (1996). Glucose intolerance but normal satiety in mice with a null mutation in the glucagon-like peptide 1 receptor gene. Nat. Med. *2*, 1254-1258. 10.1038/nm1196-1254.

S3. Wong, C.K., Yusta, B., Koehler, J.A., Baggio, L.L., McLean, B.A., Matthews, D., Seeley, R.J., and Drucker, D.J. (2022). Divergent roles for the gut intraepithelial lymphocyte GLP-1R in control of metabolism, microbiota, and T cell-induced inflammation. Cell Metab. *34*, 1514-1531.e7. 10.1016/j.cmet.2022.08.003.

S4. Panjwani, N., Mulvihill, E.E., Longuet, C., Yusta, B., Campbell, J.E., Brown, T.J., Streutker, C., Holland, D., Cao, X., Baggio, L.L., and Drucker, D.J. (2013). GLP-1 receptor activation indirectly reduces hepatic lipid accumulation but does not attenuate development of atherosclerosis in diabetic male ApoE-/- mice. Endocrinology *154*, 127-139. 10.1210/en.2012-1937.